
Beyond Visual Appearances: Privacy-sensitive Objects Identification via Hybrid Graph Reasoning

Zhuohang Jiang^{1†}, Bingkui Tong^{1†}, Xia Du², Ahmed Alhammedi³, Jizhe Zhou^{1,4*}

¹Sichuan University

²Xiamen University of Technology

³Mohamed Bin Zayed University for Humanities

⁴Engineering Research Center of Machine Learning and Industry Intelligence, MOE, China

Abstract

The Privacy-sensitive Object Identification (POI) task allocates bounding boxes for privacy-sensitive objects in a scene. The key to POI is settling an object's privacy class (privacy-sensitive or non-privacy-sensitive). In contrast to conventional object classes which are determined by the visual appearance of an object, one object's privacy class is derived from the scene contexts and is subject to various implicit factors beyond its visual appearance. That is, visually similar objects may be totally opposite in their privacy classes. To explicitly derive the objects' privacy class from the scene contexts, in this paper, we interpret the POI task as a visual reasoning task aimed at the privacy of each object in the scene. Following this interpretation, we propose the PrivacyGuard framework for POI. PrivacyGuard contains three stages. i) Structuring: an unstructured image is first converted into a structured, heterogeneous scene graph that embeds rich scene contexts. ii) Data Augmentation: a contextual perturbation oversampling strategy is proposed to create slightly perturbed privacy-sensitive objects in a scene graph, thereby balancing the skewed distribution of privacy classes. iii) Hybrid Graph Generation & Reasoning: the balanced, heterogeneous scene graph is then transformed into a hybrid graph by endowing it with extra "node-node" and "edge-edge" homogeneous paths. These homogeneous paths allow direct message passing between nodes or edges, thereby accelerating reasoning and facilitating the capturing of subtle context changes. Based on this hybrid graph, we further construct a hybrid graph attention network for reasoning. This network employs node and semantic-level attention with an imbalance compensation loss, ensuring fast and precise POI outcomes. Considering the diverse privacy perceptions among individuals, we further yield two comprehensive POI benchmarks from public-available data by employing multiple human annotators and synthesizing from government-censored TV shows. Exhaustive experimentation on established and our benchmarks evidenced that PrivacyGuard significantly outperforms current models on all evaluative criteria, achieving remarkable accuracy in detecting privacy-sensitive objects across diverse scenes.

1 Introduction

With the rapid development of social media platforms, enormous numbers of people share their own images and videos online[1, 2]. Simultaneously, advancements in generative artificial intelligence

*Corresponding author: Jizhe Zhou (jzzhou@scu.edu.cn)

†Equal contribution.

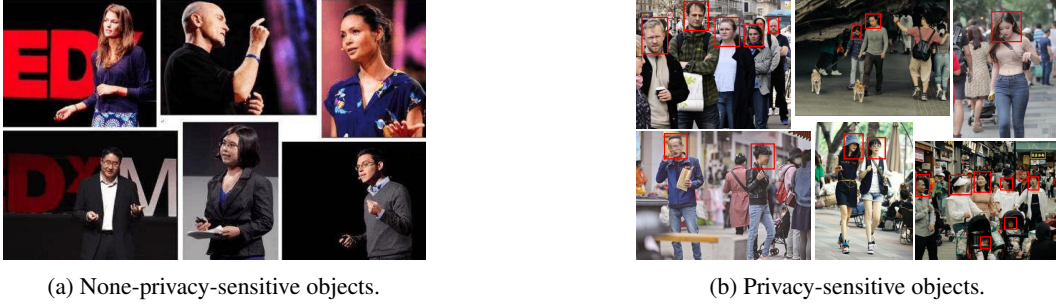


Figure 1: The privacy of an object requires reasoning based on the category of the object and information about the environment in which the object is located. The person in Figure (a) is wearing a suit and standing on a lectern to give a speech, so the facial information of the speaker is not privacy-sensitive information, while the person in Figure (b) is in the street and is dressed casually, so the facial information of the Figure is privacy-sensitive information. The privacy of the same facial information in different environments is different and needs to be determined by inference.

technologies have led to a surge in AI-generated images and videos[3, 4]. This phenomenon has significantly increased both the volume and complexity of visual content posted on social platforms, creating unprecedented challenges for privacy safeguarding. Facing massive and complex visual content, manual censorship becomes impractical, necessitating automated privacy safeguarding mechanisms[5, 6]. Currently, automated privacy safeguarding mechanisms are learning-driven and adopt an "identification-then-filtering" paradigm, which assembles privacy filters[7] on top of the privacy identification results[8]. The crux, however, lies in the granularity of application. Most privacy filters, such as face de-identification models[9] and privacy-sensitive object pixelation models[4], are performed at the object-level. Then, the identification models must also attain the same level of precision. Regrettably, current models merely achieve image-level privacy detection or identification[10, 11]. The object-level privacy identification task is left totally unresolved, thereby hindering the practical implementation of learning-driven privacy safeguarding in visual content. Hence, the Privacy-sensitive Object Identification (POI) task, which allocates the bounding boxes to privacy-sensitive objects in a scene, becomes vital to safeguarding privacy within today's visual content.

Existing object detection models can correctly locate the objects in an image[[12, 13, 14]. However, determining the privacy classes (privacy-sensitive or non-privacy-sensitive)[4] of located objects cannot be simply solved by migrating existing object detection methods to POI tasks. Because conventional object classes, such as "cat" and "dog," are primarily determined by the object's visual appearance, such as color, shape, texture, etc. Scene contexts are commonly neglected in conventional object detection tasks. While in POI, the privacy class of an object is derived from the scene contexts and influenced by various implicit factors beyond its visual appearance. For instance, as illustrated in Figure 1, the privacy of individuals' faces is derived from their roles in the scene rather than the visual features of their faces. In Figure 1a, these people are dressing formal suits, waving their hands and speaking from the lectern. Therefore, we can infer that they are speakers and their facial information gains voluntary nature of engaging in public discourse. Whereas in Figure 1b, the individuals are dressing casually and strolling on the street. Thereby, we can infer that they are ordinary passersby, rendering their facial information privacy-sensitive. As a result, visually similar objects can have opposite privacy classes due to slight differences in scene contexts or implicit factors beyond their visual appearances. Determining an object's privacy class requires comprehensive reasoning based on the scene contexts rather than merely capturing its visual features.

So far, privacy identification algorithms [11, 15, 16, 17] all follow the conventional object detection architectures, which primarily focus on visual appearances and lack the reasoning ability to derive objects' privacy classes from contexts. Consequently, current privacy identification algorithms merely achieve image-level privacy identification and are incapable of handling object-level privacy-sensitive identification. As yet, POI task is totally unresolved.

To explicitly equip the model with reasoning abilities for deriving privacy-sensitive objects from a scene, in this paper, we interpret POI as a visual reasoning task that reasons all objects' privacy classes in a scene and showcases the privacy-sensitive ones through bounding boxes. Based on this

interpretation, we propose the PrivacyGuard framework for POI. The PrivacyGuard workflow consists of three main stages: Structuring, Data Augmentation, and Hybrid Graph Generation & Reasoning. Since visual reasoning typically relies on structured data, such as graphs[18], PrivacyGuard first leverages scene graph generation[19] models to convert an image into a scene graph. Objects in the image are nodes in the scene graph, and relations between objects are the edges. The scene graph formulates a structured presentation of an unstructured image and embeds rich scene contexts. As a single image contains various objects as well as relations between objects, this scene graph is heterogeneous. After structuring, the distribution of privacy-sensitive and non-privacy-sensitive nodes requires balancing. Privacy-sensitive objects are commonly far less than the non-privacy-sensitive ones in a scene. This imbalanced class distribution will cause model underfits to the minor yet important privacy-sensitive objects. Consequently, in the second stage of PrivacyGuard, we propose a contextual perturbation oversampling strategy to perturb the context and create new, slightly modified privacy-sensitive objects in the scene graph, thereby generating more balanced heterogeneous scene graphs[20]. Compared to homogeneous graphs, heterogeneous graphs contain more scene information, but slow down the inference process. To achieve both the inference speed of homogeneous graphs and the rich scene information of heterogeneous graphs, in the third stage of PrivacyGuard, we transform the balanced heterogeneous scene graph into a hybrid graph by adding additional homogeneous paths (including "node-node" and "edge-edge" paths). These homogeneous paths facilitate direct message passing between nodes or edges, accelerating the reasoning speed and capturing subtle contextual changes. Building on this hybrid graph, we further develop a Hybrid Graph Reasoning (HGR) network. This network employs node and semantic-level attention mechanisms combined with imbalance compensation loss during the reasoning process for node privacy classes, ensuring fast and accurate POI results.

Besides the PrivacyGuard framework, considering existing privacy datasets are small in scale and overlooked the problem that different people may have diverse privacy perceptions or preferences[21, 22], we created two comprehensive POI benchmark datasets to advance POI research. Our dataset creation process adheres to strict ethical guidelines, with data from publicly available data sources. For dataset annotation, given that different people may have different perceptions regarding the same object’s privacy class, we hired multiple human annotators to label the publicly available data and filtered out inconsistent annotations by selecting parts with generally agreed opinions to ensure the annotation quality. Moreover, we also build synthesized data from legally publicly available television programs reviewed by the government. This synthesizing approach generates a large volume of diverse scenes containing privacy-sensitive objects, greatly enhancing the diversity of the datasets.

Extensive experimental tests on existing benchmark datasets and our newly proposed benchmarks demonstrated that the PrivacyGuard framework significantly outperformed existing models across all evaluation metrics, particularly in diverse and complex scenes. The outstanding performance of PrivacyGuard will drive progress in the POI field.

In short, our main contributions are summarized as follows:

- We interpret the POI task as the task of visual reasoning for each object’s privacy in a scene. We can build model which can explicitly derive objects’ privacy classes from contextual information beyond their visual appearances.
- Following our proposed new POI task interpretation, we proposed the PrivacyGuard framework, which includes three stages: Scene Graph Structuring, Contextual Perturbation Oversampling Technique based Data Augmentation, and Hybrid Graph Generation & Reasoning.
- We created two comprehensive POI benchmark datasets using publicly available data. The data collection and processing procedures address the issue of diverse privacy perceptions and the traditional privacy datasets’ difficulty in scaling up while strictly adhering to legal regulations. These datasets fill the dataset gap in the field.

2 Method

In exploring the Privacy Image Protection task, we have found that there are currently no privacy-sensitive identification models capable of achieving object-level precision. Additionally, the field of privacy object detection has not yet employed visual reasoning techniques to consider contextual

information. Due to these challenges, current work in this area is relatively sparse, making it difficult to find directly related work. Therefore, we have saved those less related works in Appendix A.1.

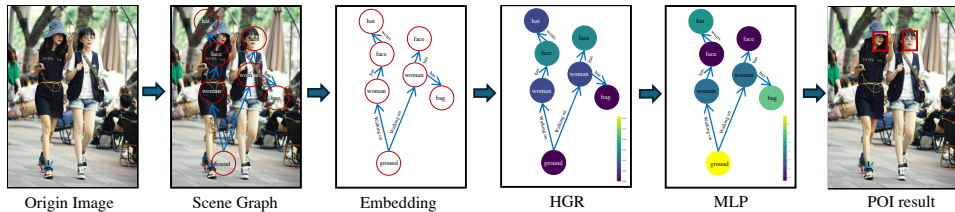


Figure 2: The workflow of the PrivacyGuard framework.

Following our novel interpretation of POI, we introduce the PrivacyGuard framework, a generalized privacy-sensitive object identification framework. As shown in Figure 2, the PrivacyGuard framework consists of three stages.

In the first stage, we employ a scene generation model as the backbone for feature extraction, leveraging its pre-trained weights to transform unstructured image data into structured heterogeneous scene graph data. By constructing a scene graph, the PrivacyGuard framework attains the contextual information within the image. However, the graph may have an imbalanced distribution of privacy-sensitive and non-privacy-sensitive nodes.

In the second stage, we propose a contextual perturbation oversampling strategy to address this imbalance. This approach generates balanced heterogeneous scene graphs by creating slightly deviated privacy-sensitive nodes in the scene graph.

After building the scene graphs, in the third stage, PrivacyGuard transforms the heterogeneous graph into a hybrid graph by adding additional homogeneous paths, including "node-node" and "edge-edge" paths. These paths facilitate direct message passing between nodes or edges and capture subtle contextual changes. Based on the hybrid graph, we propose the Hybrid Graph Reasoning (HGR) network. HGR reasons about objects' privacy-sensitive classes beyond their visual appearances by using a node and semantic-level attention mechanism along with imbalance compensation loss. Ultimately, PrivacyGuard determines objects' privacy-sensitive classes.

2.1 Structuring

We employed two advanced pre-trained models, Casual-MOTIFS[23] and ReI TR[24], to obtain contextual scene information from images. The Casual-MOTIFS model utilizes causal inference techniques to generate fair and unbiased scene graphs, demonstrating excellent performance in object recognition and relationship construction. Moreover, it effectively reduces bias by thoroughly analyzing the causal relationships within images, producing accurate and objective scene graphs, which is crucial for identifying privacy-sensitive objects. In the open-source scene graph generation models, Casual-MOTIFS[23] is considered one of the leading choices due to its outstanding performance and fairness. On the other hand, the ReI TR[24] model adopts an end-to-end Transformer architecture to extract scene information. This design that not only simplifies the model structure but also enhances efficiency. We can comprehensively prove our idea's validity by combining these two significantly different models.

The principle of scene graph generation can be summarized as follows: First, multiple region proposals are generated using Faster R-CNN[25], then bidirectional LSTM[26] or Transformer[27] models are used to process and extract object categories and scene information, ultimately constructing a scene graph. The scene graphs generated by these two models contain two types of information: the features of the nodes o and the relationships between the nodes r . Traditional homogeneous graph networks cannot represent both the node and the relationship information simultaneously, while heterogeneous graphs can include various types of connections and nodes. Therefore, we consider the relationship in the generated scene graph as a new kind of node as well, thus constituting a heterogeneous graph consisting of (o, r) , where o is the Category Node and r is the Relation Node.

2.2 Data Augmentation

Due to the smaller number of privacy-sensitive nodes compared to non-privacy-sensitive nodes in the dataset, effective training is challenging. Therefore, we need to balance the dataset by adopting a **contextual perturbation oversampling technique**. The privacy-sensitivity of an object is mainly influenced by one or two key relationships and their categories. Placing objects with the same features in the vicinity of the context of privacy-sensitive objects, i.e., copying the features of privacy-sensitive nodes and most of their relationships and appropriately modifying some relationship features, will not significantly alter the privacy-sensitive characteristics in most cases. Although a small portion of the augmented data might experience changes in privacy-sensitivity due to modifications of critical relationships, the vast majority of the privacy-sensitivity remains unchanged. Thus, this approach can increase the diversity of the dataset while ensuring the correctness of most augmented data.

Based on the above theory, during the data augmentation process using the contextual perturbation oversampling algorithm, we randomly select some privacy-sensitive nodes in the graph and replicate their node features. Then, we use a single-layer random walk method to select the connections, ensuring that the replicated nodes retain most of the original nodes' connections while randomly introducing some incorrect connections (e.g., more or fewer connections) and randomly correcting these connections, thereby achieving dataset augmentation.

2.3 Hybrid Graph Generation & Reasoning

The Hybrid Graph Reasoning consists of three steps: **1.** Generating a hybrid graph from a heterogeneous graph. **2.** Applying node-level attention to identical node-paths. **3.** Applying semantic-level attention to different node-paths to generate privacy-sensitive feature vectors for each node, which are then used to generate privacy-sensitive values through an MLP.

This network leverages node and semantic-level attention, combined with an imbalance compensation loss, to deliver swift and precise POI results.

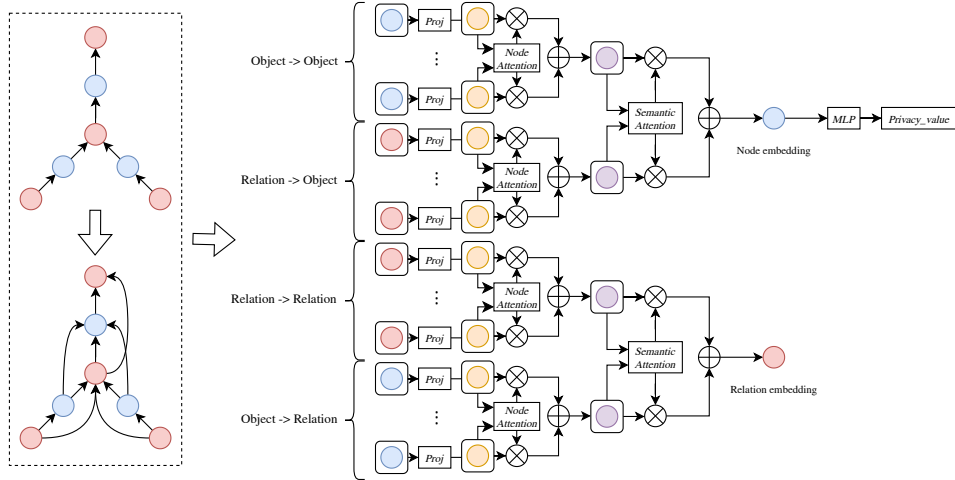


Figure 3: Overview diagram of the third stage of PrivacyGuard: Hybrid Graph Generation & Reasoning, which is responsible for transmitting information between nodes, conducting inference, and ultimately determining whether it is a privacy-sensitive node.

2.3.1 Hybrid Graph Generation

Heterogeneous graph neural networks have high computational accuracy and can transfer node information through $o \rightarrow r \rightarrow o$, thus enabling contextual inference. However, due to the low efficiency of heterogeneous graph neural networks and the loss of information caused by indirectly transferring information between nodes, we added the connection $o_i \rightarrow r \rightarrow o_j$ when there exists $o_i \rightarrow r \rightarrow o_j$; and when there exists $r_i \rightarrow o \rightarrow r_j$, we added the connection $r_i \rightarrow r_j$. Thus, homomorphic structures are added in the case of heterogeneous graphs. These homogeneous paths allow direct message passing between nodes or edges, accelerating inference and helping capture

subtle contextual variations, thereby improving the efficiency and accuracy of node information acquisition.

In this way, the connection structure of nodes is increased from the original two paths to four paths.

$$(o \rightarrow r, r \rightarrow o) \Rightarrow (o \rightarrow r, r \rightarrow o, r \rightarrow r, o \rightarrow o)$$

2.3.2 Node-Level Attention

We consider four kinds of metapaths in the generated heterogeneous graph, namely $(o \rightarrow r, r \rightarrow o, r \rightarrow r, o \rightarrow o)$. For each metapath, we perform an attention convolution operation of the graph nodes to generate feature vectors for different metapaths.

First, for the category nodes o and r , we perform feature transformations using the feature matrices W_1 and W_2 , respectively:

$$\begin{cases} \hat{o}_i = W_1 \cdot o_i \\ \hat{r}_i = W_2 \cdot r_i \end{cases}$$

Then, for nodes on the same path, we perform the attention operation. For the pair of nodes $N_i \rightarrow M_j$ on the path $N \rightarrow M$, we compute the attention information $e_{M_j}^{N_i}$:

$$e_{M_j}^{N_i} = att_{node}(N_i, M_j, N \rightarrow M) \quad \text{where } (N_i, M_i = \hat{o}_i \text{ or } \hat{r}_i)$$

Next, a Softmax operation is performed on the attention information $e_{M_j}^{N_i}$ to obtain the weight values $\alpha_{M_j}^{N_i}$:

$$\alpha_{M_j}^{N_i} = soft \max \left(e_{M_j}^{N_i} \right) = \frac{\exp \left(\sigma \left(a_M^N \cdot (N_i \otimes M_j) \right) \right)}{\sum_{m \in P_M^{N_i}} \exp \left(\sigma \left(a_M^N \cdot (N_i \otimes M_m) \right) \right)}$$

Finally, for each connection in the same path, we multiply the feature vector M_m by the corresponding attentional weight and add them together to generate the feature vector. For each node N_i , we obtain a set of feature vectors $\{z_{\kappa_1}^{N_i}, z_{\kappa_2}^{N_i}, \dots, z_{\kappa_i}^{N_i}\}$, where $\kappa(M \rightarrow N)$ denotes the path. $z_M^{N_i}$ denotes the node features after the superposition of attentional weights, $\alpha_{M_m}^{N_i}$ denotes the attentional weight of each connection, and M_m denotes the feature vector of the connection:

$$z_M^{N_i} = \sigma \left(\sum_{m \in P_M^{N_i}} \alpha_{M_m}^{N_i} \cdot M_m \right)$$

2.3.3 Semantic-Level Attention

We synthesize an attention network by synthesizing semantics with the same node categories but different meta-paths, assigning different parameters to different meta-paths. This is done so that category nodes can collect features of neighboring relations and also access features of neighboring category nodes. In this way, we can infer the information about the contextual in which the node is located from the neighboring features and relationship nodes, and finally generate an embedding vector for each node.

First, for different path features $z_{o_i}^c, z_{o_i}^r, z_{r_i}^c, z_{r_i}^r$, we perform the feature transformations using the feature matrices $W_3, W_4, W_5,$ and W_6 respectively:

$$\begin{cases} z_{\hat{o}_i}^c = W_3 \cdot z_{o_i}^o \\ z_{\hat{o}_i}^r = W_4 \cdot z_{o_i}^r \\ z_{\hat{r}_i}^c = W_5 \cdot z_{r_i}^o \\ z_{\hat{r}_i}^r = W_6 \cdot z_{r_i}^r \end{cases}$$

Then, the attention weights w_{κ_i} are computed by calculating the information of the attention weights between different paths, and then using these weights to perform a normalization operation to compute the attention weights β_{κ_i} .

$$w_{\kappa_i} = \frac{1}{|\mathcal{V}|} \sum_{j \in \mathcal{V}} q^T \cdot \tanh(W \cdot z_{\kappa_i}^{N_j} + b) \beta_{\kappa_i} = \frac{\exp(w_{\kappa_i})}{\sum \exp(w_{\kappa_i})}$$

Then, for the feature vectors derived in the previous step, the attention weight β_{κ_i} operation is applied on different paths, which finally generates the feature information Z^{N_i} corresponding to each node.

$$Z^{N_i} = \sum \beta_{\kappa_i} \cdot z_{\kappa_i}^{N_i}$$

We use multi-layer hybrid graph attention neural networks for information transfer to gather information about nodes and relationships further away. Subsequently, each embedding vector is processed by a multilayer perceptron (MLP), and finally the output privacy confidence is used to determine whether the node is a privacy-sensitive node or not. Where $is_privacy_{N_i}$ represents the privacy-sensitive degree of node N_i .

$$is_privacy_{N_i} = \text{sigmoid}(W \cdot Z^{N_i} + b)$$

3 Experiments

3.1 Dataset Introduction

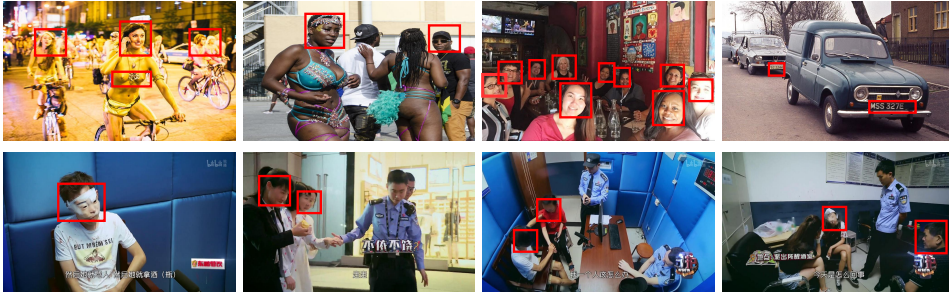


Figure 4: The Figure shows photos in our two datasets. **First Row:** PRIVACY1000. **Second Row:** MOSAIC.

In this paper, we introduce two benchmark datasets for Privacy-sensitive Object Identification (POI): **MOSAIC** and **PRIVACY1000**. The **MOSAIC** dataset comprises images we collected and processed from government-censored TV programs. The **PRIVACY1000** dataset includes images we gathered and manually annotated from Flickr[28]. An overview of these datasets is presented in Figure 4. Throughout the data collection and annotation process, we strictly adhered to privacy protection laws and regulations, thereby contributing valuable data resources to the field of POI.

3.1.1 MOSAIC

The **MOSAIC** dataset comprises a total of 13,384 images, encompassing various categories of privacy-sensitive objects such as people’s faces, body parts, instances of bloody violence, transcripts, license plates, slogans, etc. The construction of the **MOSAIC** dataset involved the following steps:

1. **Privacy-Sensitive Images Collection:** We hypothesized that mosaic regions in images usually indicate privacy-sensitive objects and thus extracted frames containing mosaics from dozens of hours of video(Guardians of Liberation West).
2. **Mosaic Localization:** Using YOLO[29], we accurately localized mosaic areas in the images. Then, we removed the mosaics while recording their information, including index numbers and precise location coordinates.

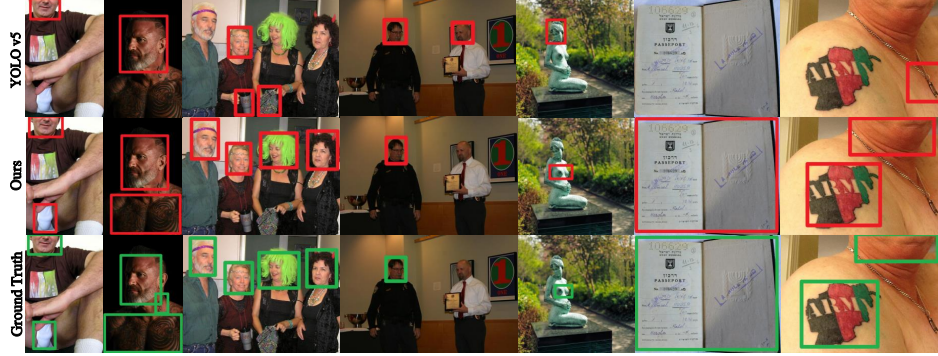


Figure 5: Partial results of PrivacyGuard, compared with Ground Truth and YOLO v5. More model result comparisons are in the appendix Figure10.

3. **Removed Content Restoration:** To avoid directly collecting factual and privacy-sensitive information, we employed Artificial Intelligence Generated Content technology [30] to restore the portions of the images where mosaics were removed. This step allows us to effectively gather privacy-related images without accessing actual privacy-sensitive data.

The construction of the MOSAIC dataset was conducted in strict accordance with relevant laws and regulations, ensuring that there were no instances of privacy violations. The illustration of the dataset collection process is in the appendix Figure6

3.1.2 PRIVACY1000

The **PRIVACY1000** dataset consists of 1000 real-world images featuring a variety of privacy-sensitive objects such as body parts, human faces, distinctive clothing, bloody photos, political slogans, and license plate messages. All data was manually annotated. To address subjective differences in privacy perceptions, we adopted a majority-rule approach. If more than half of the annotators considered an object privacy-sensitive, it was categorized as such. Out of respect for privacy, the PRIVACY1000 dataset is not publicly available.

3.2 Experimental Setup

In our experimental setup, we used the PRIVACY1000 dataset for model training and the MOSAIC dataset to test the model’s generalization capabilities. We randomly partitioned the PRIVACY1000 dataset, allocating 80% as the training set and 20% as the validation set. For our baselines, we selected YOLOv5 [29] and Faster RCNN [31], both of which have demonstrated excellent performance in traditional object detection tasks.

3.3 Experiment Results

In this paper we compared the performance of traditional object detection models (YOLOv5[29] and Faster-RCNN[31]) and PrivacyGuard using different scene graph generation modules (Casual-MOTIFS[23] and ReI TR[24]) on the MOSAIC and PRIVACY1000 datasets. It is found that the traditional models perform poorly on the privacy object detection task that requires inference beyond visual appearances. In contrast, the Casual-MOTIFS+HGR and ReI TR+HGR models identify

Table 1: Experimental results for the two privacy datasets using different algorithms.

Methods	PRIVACY1000			MOSAIC		
	Precision	Recall	F1 Score	Precision	Recall	F1 Score
Faster-RCNN[31]	0.7192	0.4981	0.5886	0.2917	0.2662	0.2784
YOLOv5[29]	0.8667	0.6634	0.7515	0.4323	0.3543	0.3894
ReI TR[24]+HGR	0.8975	0.8798	0.8886	0.6870	0.7174	0.7019
PrivacyGuard	0.9723	0.9165	0.9436	0.9349	0.9546	0.9447

Table 2: The table below shows experiment results for ablation experiments. S, DA, and GR stand for the three stages: Structuring, Data Augmentation, and Graph Reasoning, respectively.

Methods	Modify			Precision	Recall	F1 score
	S	DA	GR			
RelTR[24]+CPOS+GCN[33]	✗	✓	✗	0.8634	0.8723	0.8678
RelTR[24]+CPOS+GAT[32]	✗	✓	✗	0.8692	0.8654	0.8673
RelTR[24]+CPOS+HGR	✗	✓	✓	0.8975	0.8798	0.8886
Casual-MOTIFS[23]+CPOS+GCN[33]	✓	✓	✗	0.9011	0.8786	0.8902
Casual-MOTIFS[23]+CPOS+GAT[32]	✓	✓	✗	0.9552	0.8697	0.9104
Casual-MOTIFS[23]+SMOTE[34]+HGR	✓	✗	✓	0.8872	0.9344	0.9102
PrivacyGuard	✓	✓	✓	0.9723	0.9165	0.9436

privacy-sensitive objects more accurately. Even with RelTR’s suboptimal scene graph construction ability, HGR significantly outperforms traditional object detection models on POI tasks. The Casual-MOTIFS+HGR model outperforms the baseline model on all evaluation metrics by constructing a hybrid graph and performing inference, showing superior performance in the privacy object detection task.

In Figure 5, the YOLOv5 model successfully identifies apparent privacy-sensitive features such as faces and hair. However, it performs poorly when detecting privacy-sensitive objects that require inference, such as the people in different roles on the award podium. For example, in the fourth image of Figure 5, YOLOv5 detects faces but fails to recognize that facial information is not all privacy-sensitive in the given contexts. However, Our **PrivacyGuard** framework, accurately interprets the scene contexts and demonstrates superior reasoning ability in privacy-sensitive object detection.

3.4 Ablation Experiments

In order to gain a deeper understanding of the contribution of each module in the HGR model to performance, we conducted several ablation experiments. To explore the impact of heterogeneous graph structure, we replace HGR with GAT[32], which prevents the model from capturing information about relationships between objects in the scene. Based on this, we further replace HGR with GCN[33] to investigate the impact of the attention mechanism. Meanwhile, to demonstrate the effectiveness of our proposed contextual perturbation oversampling strategy (CPOS), we compare its performance with the Synthetic Minority Over-Sampling Technique (SMOTE)[34].

The poor performance of Casual-MOTIFS[23]+GCN[33] can be attributed to the fact that the homography it uses cannot capture the complex relationships between objects in the scene effectively. In addition, the model’s inference process relies on convolutional operations rather than attentional mechanisms, limiting the model’s perceptual range and making it challenging to capture long-range dependencies. Although Casual-MOTIFS[23]+GAT[32] introduces an attentional mechanism, its performance is still limited because it also performs implicit inference based on homography. In contrast, the HGR model constructs a heterogeneous graph to capture the scene information comprehensively and uses the self-attention mechanism for inference based on it, thus outperforming other methods in terms of performance. Meanwhile, the use of SMOTE is not as effective as our contextual perturbation oversampling strategy, which further proves the effectiveness of our proposed method.

4 Conclusion

This study provides insights into the privacy-sensitive object identification (POI) task, which aims to assign bounding boxes to privacy-sensitive objects in a scene. Unlike traditional object classes determined based on visual appearance, privacy classes must be determined based on scene contexts and implicit factors beyond visual appearance. For this reason, we interpret the POI task as a visual inference task for the privacy of each object in the scene. Thus, we propose the PrivacyGuard framework to solve the POI problem, which consists of three stages: first, Structuring stage, which converts unstructured images into heterogeneous scene graphs embedded with rich contextual information; second, data augmentation stage, which creates slightly biased privacy-sensitive objects through

bias over-sampling techniques in order to balance the data distributions; and finally, hybrid graph generation & inference stage, which transforms the balanced heterogeneous scene graphs into hybrid graphs with additional isomorphic paths, capturing subtle contextual changes, and constructing hybrid graph attention networks for accurate inference. Considering the variability of privacy perception, we create two POI benchmark datasets, PRIVACY1000 and MOSAIC, from multiple manually labeled and government-censored TV program data. Experimental results show that PrivacyGuard achieves 97% accuracy on the PRIVACY1000 dataset and significantly outperforms existing models on all evaluation criteria, realizing excellent privacy-sensitive object detection accuracy.

References

- [1] Oded Nov, Mor Naaman, and Chen Ye. Motivational, structural and tenure factors that impact online community photo sharing. In *Proceedings of the International AAAI Conference on Web and Social Media*, volume 3, pages 138–145, 2009.
- [2] Jizhe Zhou and Chi-Man Pun. Personal privacy protection via irrelevant faces tracking and pixelation in video live streaming. *IEEE Transactions on Information Forensics and Security*, 16:1088–1103, 2020.
- [3] Nuha Aldausari, Arcot Sowmya, Nadine Marcus, and Gelareh Mohammadi. Video generative adversarial networks: A review. *ACM Comput. Surv.*, 55(2), jan 2022.
- [4] Jizhe Zhou, Chi-Man Pun, and Yu Tong. Privacy-sensitive objects pixelation for live video streaming. In *Proceedings of the 28th ACM International Conference on Multimedia*, pages 3025–3033, 2020.
- [5] Slobodan Ribaric, Aladdin Ariyaeenia, and Nikola Pavesic. De-identification for privacy protection in multimedia content: A survey. *Signal Processing: Image Communication*, 47:131–151, 2016.
- [6] Xiaokui Shu, Danfeng Yao, and Elisa Bertino. Privacy-preserving detection of sensitive data exposure. *IEEE transactions on information forensics and security*, 10(5):1092–1103, 2015.
- [7] Tao Li and Lei Lin. Anonymousnet: Natural face de-identification with measurable privacy. In *Proceedings of the IEEE/CVF Conference on Computer Vision and Pattern Recognition (CVPR) Workshops*, June 2019.
- [8] Xinyu Zhang, Huiyu Xu, Zhongjie Ba, Zhibo Wang, Yuan Hong, Jian Liu, Zhan Qin, and Kui Ren. Privacyasst: Safeguarding user privacy in tool-using large language model agents. *IEEE Transactions on Dependable and Secure Computing*, pages 1–16, 2024.
- [9] R. Gross, L. Sweeney, F. de la Torre, and S. Baker. Model-based face de-identification. In *2006 Conference on Computer Vision and Pattern Recognition Workshop (CVPRW’06)*, pages 161–161, 2006.
- [10] Bach Ngoc Kim, Jose Dolz, Pierre-Marc Jodoin, and Christian Desrosiers. Privacy-net: An adversarial approach for identity-obfuscated segmentation of medical images, 2020.
- [11] Lam Tran, Deguang Kong, Hongxia Jin, and Ji Liu. Privacy-cnh: A framework to detect photo privacy with convolutional neural network using hierarchical features. In *Proceedings of the AAAI conference on artificial intelligence*, volume 30, 2016.
- [12] Zhuofan Zong, Guanglu Song, and Yu Liu. Detrs with collaborative hybrid assignments training, 2023.
- [13] Wenhai Wang, Jifeng Dai, Zhe Chen, Zhenhang Huang, Zhiqi Li, Xizhou Zhu, Xiaowei Hu, Tong Lu, Lewei Lu, Hongsheng Li, Xiaogang Wang, and Yu Qiao. Internimage: Exploring large-scale vision foundation models with deformable convolutions, 2023.
- [14] Weijie Su, Xizhou Zhu, Chenxin Tao, Lewei Lu, Bin Li, Gao Huang, Yu Qiao, Xiaogang Wang, Jie Zhou, and Jifeng Dai. Towards all-in-one pre-training via maximizing multi-modal mutual information, 2022.
- [15] Xin Jin, Yuhui Wang, and Xiaoyang Tan. Pornographic image recognition via weighted multiple instance learning. *IEEE Transactions on Cybernetics*, 49(12):4412–4420, 2019.
- [16] Mohamed Moustafa. Applying deep learning to classify pornographic images and videos, 2015.
- [17] Ashwini Tonge and Cornelia Caragea. Image privacy prediction using deep neural networks, 2019.
- [18] Justin Johnson, Bharath Hariharan, Laurens Van Der Maaten, Li Fei-Fei, C Lawrence Zitnick, and Ross Girshick. Clevr: A diagnostic dataset for compositional language and elementary visual reasoning. In *Proceedings of the IEEE conference on computer vision and pattern recognition*, pages 2901–2910, 2017.
- [19] Guangming Zhu, Liang Zhang, Youliang Jiang, Yixuan Dang, Haoran Hou, Peiyi Shen, Mingtao Feng, Xia Zhao, Qiguang Miao, Syed Afaq Ali Shah, et al. Scene graph generation: A comprehensive survey. *arXiv preprint arXiv:2201.00443*, 2022.
- [20] Xiao Wang, Deyu Bo, Chuan Shi, Shaohua Fan, Yanfang Ye, and S Yu Philip. A survey on heterogeneous graph embedding: methods, techniques, applications and sources. *IEEE Transactions on Big Data*, 9(2):415–436, 2022.

- [21] Zhenyu Wu, Haotao Wang, Zhaowen Wang, Hailin Jin, and Zhangyang Wang. Privacy-preserving deep action recognition: An adversarial learning framework and a new dataset. *IEEE Transactions on Pattern Analysis and Machine Intelligence*, 44(4):2126–2139, 2020.
- [22] Chenye Zhao, Jasmine Mangat, Sujay Koujalgi, Anna Squicciarini, and Cornelia Caragea. Privacyalert: A dataset for image privacy prediction. In *Proceedings of the International AAAI Conference on Web and Social Media*, volume 16, pages 1352–1361, 2022.
- [23] Kaihua Tang, Yulei Niu, Jianqiang Huang, Jiaxin Shi, and Hanwang Zhang. Unbiased scene graph generation from biased training. In *Proceedings of the IEEE/CVF conference on computer vision and pattern recognition*, pages 3716–3725, 2020.
- [24] Yuren Cong, Michael Ying Yang, and Bodo Rosenhahn. Reltr: Relation transformer for scene graph generation. *IEEE Transactions on Pattern Analysis and Machine Intelligence*, 2023.
- [25] Shaoqing Ren, Kaiming He, Ross B. Girshick, and Jian Sun. Faster R-CNN: towards real-time object detection with region proposal networks. *CoRR*, abs/1506.01497, 2015.
- [26] Shu Zhang, Dequan Zheng, Xinchun Hu, and Ming Yang. Bidirectional long short-term memory networks for relation classification. In *Proceedings of the 29th Pacific Asia conference on language, information and computation*, pages 73–78, 2015.
- [27] Ashish Vaswani, Noam Shazeer, Niki Parmar, Jakob Uszkoreit, Llion Jones, Aidan N Gomez, Łukasz Kaiser, and Illia Polosukhin. Attention is all you need. *Advances in neural information processing systems*, 30, 2017.
- [28] Sergej Zerr, Stefan Siersdorfer, Jonathon Hare, and Elena Demidova. Privacy-aware image classification and search. In *Proceedings of the 35th international ACM SIGIR conference on Research and development in information retrieval*, pages 35–44, 2012.
- [29] Joseph Redmon, Santosh Divvala, Ross Girshick, and Ali Farhadi. You only look once: Unified, real-time object detection. In *Proceedings of the IEEE conference on computer vision and pattern recognition*, pages 779–788, 2016.
- [30] Robin Rombach, Andreas Blattmann, Dominik Lorenz, Patrick Esser, and Björn Ommer. High-resolution image synthesis with latent diffusion models. In *Proceedings of the IEEE/CVF conference on computer vision and pattern recognition*, pages 10684–10695, 2022.
- [31] Shaoqing Ren, Kaiming He, Ross Girshick, and Jian Sun. Faster r-cnn: Towards real-time object detection with region proposal networks. *Advances in neural information processing systems*, 28, 2015.
- [32] Petar Velickovic, Guillem Cucurull, Arantxa Casanova, Adriana Romero, Pietro Lio, Yoshua Bengio, et al. Graph attention networks. *stat*, 1050(20):10–48550, 2017.
- [33] Thomas N Kipf and Max Welling. Semi-supervised classification with graph convolutional networks. *arXiv preprint arXiv:1609.02907*, 2016.
- [34] Kevin W. Bowyer, Nitesh V. Chawla, Lawrence O. Hall, and W. Philip Kegelmeyer. SMOTE: synthetic minority over-sampling technique. *CoRR*, abs/1106.1813, 2011.
- [35] Anne Adams and Martina Angela Sasse. Privacy in multimedia communications: Protecting users, not just data. In *People and computers XV—interaction without frontiers: Joint Proceedings of HCI 2001 and IHM 2001*, pages 49–64. Springer, 2001.
- [36] Victoria Bellotti. Design for privacy in multimedia computing and communications environments. *Technology and privacy: The new landscape*, pages 63–98, 1998.
- [37] Rufai Yusuf Zakari, Jim Wilson Owusu, Hailin Wang, Ke Qin, Zaharaddeen Karami Lawal, and Yuezhou Dong. Vqa and visual reasoning: An overview of recent datasets, methods and challenges, 2022.

A Appendix / supplemental material

A.1 Related Work

A.1.1 Privacy Image Protection

With the rapid growth of image data and the persistent risk of personal privacy information leakage, safeguarding users' privacy image information has become an urgent challenge in computer science and information security[35, 36]. This challenge has attracted widespread attention and relentless efforts from numerous researchers. Privacy image protection utilizes techniques such as machine learning to automatically identify and process privacy regions in images to protect user privacy effectively. Protection methods typically involve blurring, mosaic, or masking sensitive areas to ensure private regions are not directly exposed when sharing or publishing images. For example, the Privacy-CNH[11] model employs deep learning models to detect photos with privacy risks, thereby safeguarding user privacy. However, limited by the low precision of the dataset, most of the current models are limited to image-level privacy detection and less focus on object-level privacy detection models.

A.1.2 Visual Reasoning

Visual Reasoning is an important research area in computer vision and artificial intelligence, which aims to enable computers to understand the content of images and make logical inferences. This typically involves recognizing objects, attributes, and relationships between them in an image and using this information to infer dynamic changes in the scene, answer questions about the image, or predict future states. Scene graphs provide a rich semantic representation that helps solve problems requiring deep visual understanding and reasoning. Thus, Visual Reasoning based on scene graph generation (SGG) is a well-established set of Visual Reasoning methods that first extracts structured scene graphs containing objects, attributes, and relationships between them from images using SGG techniques. Then, this structured information is utilized to support higher-level reasoning tasks. Kaihua Tang et al.[23] explored how to generate unbiased scene graphs from imperfect training data and proposed a new inference algorithm. Zakari[37] described and explored Visual Reasoning based on scene graphs in detail in his paper on VQA and Visual Reasoning. However, in SGG-based Visual Reasoning, if the scale of the scene graph is insufficient, i.e., there are a limited number of objects and relations in the scene graph, it may lead to insufficient learning ability of the model to capture all the relevant information in the image, which may lead to the underfitting of the result of the Visual Reasoning. At the same time, real life is often not balanced; some categories of objects or relationships appear much more frequently than others. SGG-based Visual Reasoning cannot handle unbalanced categories well, which leads to poor reasoning results for these categories.

A.2 Dataset Introduction

In this Section, we will introduce the details of two datasets.



Figure 6: The dataset collection process for MOSAIC.

Our proposed dataset covers a variety of scenarios and includes privacy nodes of different feature classes, where the MOSAIC dataset includes more than 20,000 different privacy nodes, and the privacy1000 dataset includes more than 1,400 privacy nodes, which are categorized as shown in Table 3. We used the ResNet50 model, which was pre-trained on ImageNet1000, to extract features from

all images in the dataset. Subsequently, we employed Principal Component Analysis (PCA) to reduce these features to ten dimensions. Finally, we used 2D t-SNE and K-means clustering methods for further dimensionality reduction and visualization, with the results displayed in Figure 7. From these results, it is evident that our dataset has a balanced feature distribution, and there are clear differences between the various scenarios.

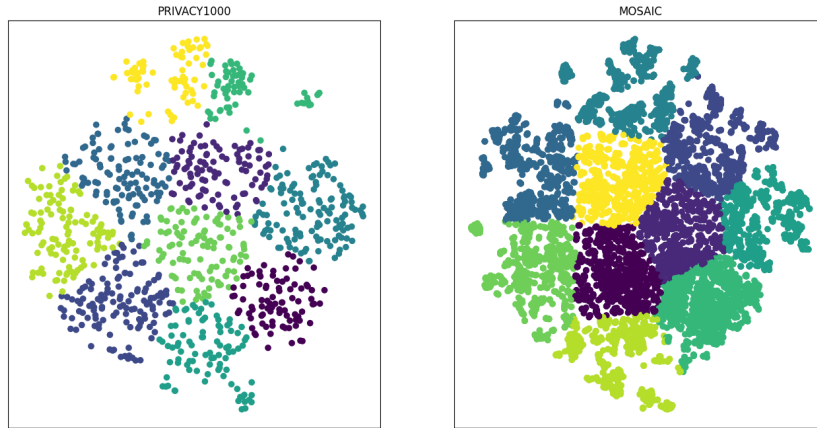


Figure 7: The Figure show the distribution of images in our dataset.

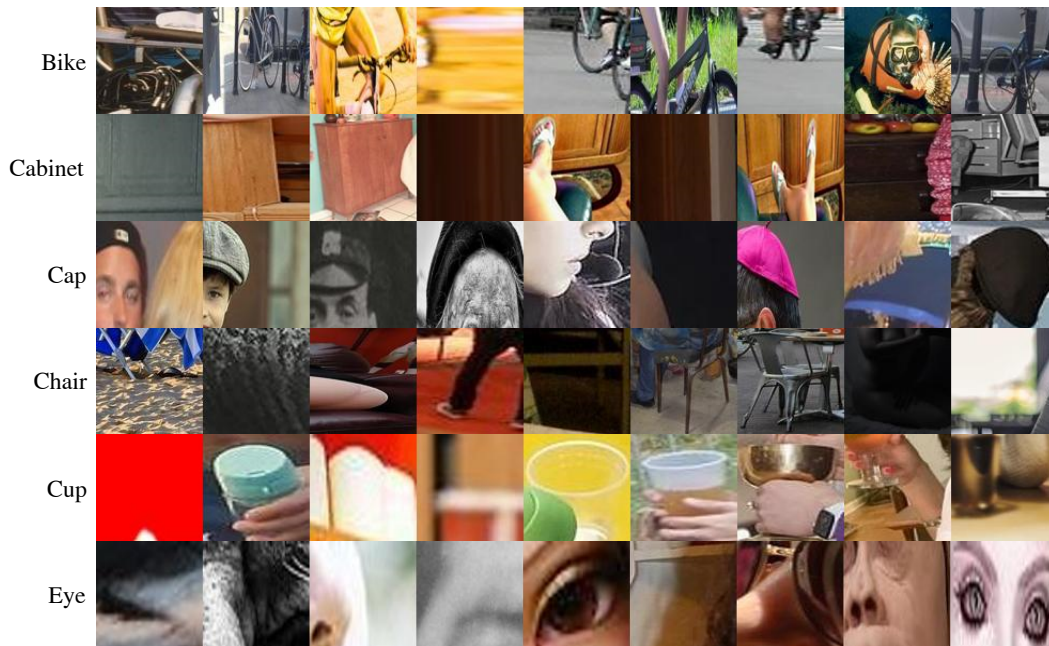


Figure 8: Some object labels in PRIVACY1000.

A.3 Robustness Experiments

To further test the robustness of PrivacyGuard, we performed each one of the following three processing methods on each image in the test set of the PRIVACY1000 dataset, and tested it on the trained PrivacyGuard model:



Figure 9: Some objects labels in MOSAIC.

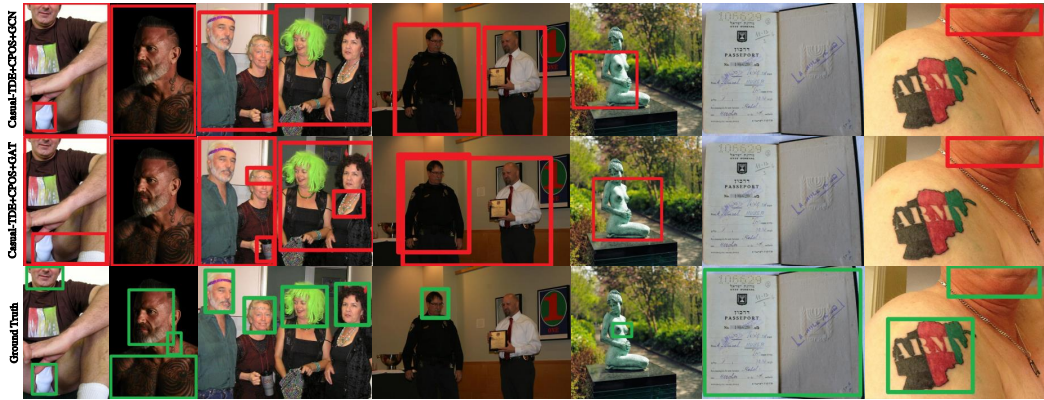


Figure 10: Partial ablation experiment results of PrivacyGuard, compared with Ground Truth.

- **Rotation:** We applied random rotation to the input image, with the rotation angle adjusted between -30 degrees and 30 degrees.
- **Masking:** We randomly selected two to three points on the input image, and then masked the area with these selected points as the center and a side length of 20 pixels.
- **Scaling:** We applied random scaling to the selected image, with the scaling ratio varying between 0.8 and 1.2.

In Table 4, we found that when PrivacyGuard faces modifications like rotation and scaling that have less impact on scene information, its performance is not greatly affected. However, when PrivacyGuard encounters changes like masking that could have a significant impact on scene information (for example, masking some key objects, leading to a loss of scene information), its overall performance drops dramatically. This proves that when PrivacyGuard analyzes the privacy sensitivity of objects, it takes into account the contextual information of the objects, and it exhibits good robustness when the contextual information of the objects does not change significantly.

Table 3: The Table below shows different categories and their explanations.

Category	Explanation
Medical	Images depicting medical conditions or visible blood, including scenes of medical treatment.
Personal information	Images containing personally identifiable information such as bank account details, home addresses, or usernames.
Other people	Pictures featuring individuals known to the photographer, bystanders, or event attendees.
Bad character/Unlawful criminal	Images related to crime scenes or depicting unlawful behaviors.
Sexual	Images displaying full or semi-nudity of individuals.
Religion/Culture	Photos revealing religious beliefs or cultural practices.
Drinking/Party	Images capturing parties, drinking, or smoking activities.
Unorganized home	Pictures showcasing messy or disorganized living spaces.
Appearance/Facial expression	Photos showing facial expressions or clothing choices that may reflect negatively on one’s character.
Violence	Photos depicting scenes of violence.

Table 4: The Table below shows experiment results for robust experiments.

Augmentation Methods	Precision	Recall	F1 score
Rotation	0.8939	0.9351	0.9141
Zoom	0.8911	0.9355	0.9128
Masking	0.8629	0.9400	0.8998
Origin	0.9723	0.9165	0.9436

A.4 Ethical Concerns

Throughout this study, we strictly adhered to relevant laws, regulations, and ethical standards to ensure the datasets’ construction and use did not involve any illegal information. Specifically, we developed two key datasets: the MOSAIC dataset and the PRIVACY1000 dataset, both of which were created without using or generating any illegal information.

The MOSAIC dataset was constructed using an innovative approach. We first collected images with mosaic processing information, then removed these mosaics and regenerated the content using an advanced Stable Diffusion model. This method avoids direct use of privacy information by reconstructing it intelligently rather than accessing the original data, ensuring the legality and ethics of our data processing.

For the PRIVACY1000 dataset, we used publicly available images from Flickr. We selected 1,000 representative real privacy images and manually labeled them. Since this dataset is based entirely on publicly accessible resources, no illegal information was involved during its collection and annotation.

By constructing and utilizing these two datasets, we ensured compliance with data processing laws and regulations and demonstrated a strong commitment to personal privacy protection. This approach not only provides valuable data resources for privacy protection research in artificial intelligence but also sets a standard for adhering to legal and ethical guidelines in future research.